

Directed, elliptic and higher order flow harmonics of protons, deuterons and tritons in Au+Au collisions at $\sqrt{s_{\text{NN}}} = 2.4$ GeV

J. Adamczewski-Musch⁵, O. Arnold^{11,10}, C. Behnke⁹, A. Belounnas¹⁷, A. Belyaev⁸, J.C. Berger-Chen^{11,10}, A. Blanco², C. Blume⁹, M. Böhmer¹¹, P. Bordalo², S. Chernenko^{8,†}, L. Chlad¹⁸, I. Ciepal³, C. Deveau¹², J. Dreyer⁷, E. Epple^{11,10}, L. Fabbietti^{11,10}, O. Fateev⁸, P. Filip¹, P. Fonte^{2,a}, C. Franco², J. Friese¹¹, I. Fröhlich⁹, T. Galatyuk^{6,5}, J.A. Garzón¹⁹, R. Gernhäuser¹¹, O. Golosov¹⁵, M. Golubeva¹³, R. Greifehagen^{7,b}, F. Guber¹³, M. Gumberidze^{5,6}, S. Harabasz^{6,4}, T. Heinz⁵, T. Hennino¹⁷, S. Hlavac¹, C. Höhne^{12,5}, R. Holzmann⁵, A. Ierusalimov⁸, A. Ivashkin¹³, B. Kämpfer^{7,b}, T. Karavicheva¹³, B. Kardan⁹, I. Koenig⁵, W. Koenig⁵, M. Kohls⁹, B.W. Kolb⁵, G. Korcyl⁴, G. Kornakov⁶, F. Kornas⁶, R. Kotte⁷, A. Kugler¹⁸, T. Kunz¹¹, A. Kurepin¹³, A. Kurilkin⁸, P. Kurilkin⁸, V. Ladygin⁸, R. Lalik⁴, K. Lapidus^{11,10}, A. Lebedev¹⁴, L. Lopes², M. Lorenz⁹, T. Mahmoud¹², L. Maier¹¹, A. Malige⁴, M. Mamaev¹⁵, A. Mangiarotti², J. Markert⁵, T. Matulewicz²⁰, S. Maurus¹¹, V. Metag¹², J. Michel⁹, D.M. Mihaylov^{11,10}, S. Morozov^{13,15}, C. Müntz⁹, R. Münzer^{11,10}, L. Naumann⁷, K. Nowakowski⁴, Y. Parpottas^{16,c}, V. Pechenov⁵, O. Pechenova⁵, O. Petukhov¹³, K. Piasecki²⁰, J. Pietraszkowski⁵, W. Przygoda⁴, K. Pysz³, S. Ramos², B. Ramstein¹⁷, N. Rathod⁴, A. Reshetin¹³, P. Rodriguez-Ramos¹⁸, P. Rosier¹⁷, A. Rost⁶, A. Rustamov⁵, A. Sadovsky¹³, P. Salabura⁴, T. Scheib⁹, H. Schuldes⁹, E. Schwab⁵, F. Scozzi^{6,17}, F. Seck⁶, P. Sellheim⁹, I. Selyuzhenkov^{5,15}, J. Siebenson¹¹, L. Silva², U. Singh⁴, J. Smyrski⁴, Yu.G. Sobolev¹⁸, S. Spataro²¹, S. Spies⁹, H. Ströbele⁹, J. Stroth^{9,5}, C. Sturm⁵, O. Svoboda¹⁸, M. Szala⁹, P. Tlusty¹⁸, M. Traxler⁵, H. Tsertos¹⁶, E. Usenko¹³, V. Wagner¹⁸, C. Wendisch⁵, M.G. Wiebusch⁵, J. Wirth^{11,10}, D. Wójcik²⁰, Y. Zanevsky^{8,†}, P. Zumbach⁵
(HADES collaboration)

¹*Institute of Physics, Slovak Academy of Sciences, 84228 Bratislava, Slovakia*

²*LIP-Laboratório de Instrumentação e Física Experimental de Partículas, 3004-516 Coimbra, Portugal*

³*Institute of Nuclear Physics, Polish Academy of Sciences, 31342 Kraków, Poland*

⁴*Smoluchowski Institute of Physics, Jagiellonian University of Cracow, 30-059 Kraków, Poland*

⁵*GSI Helmholtzzentrum für Schwerionenforschung GmbH, 64291 Darmstadt, Germany*

⁶*Technische Universität Darmstadt, 64289 Darmstadt, Germany*

⁷*Institut für Strahlenphysik, Helmholtz-Zentrum Dresden-Rossendorf, 01314 Dresden, Germany*

⁸*Joint Institute of Nuclear Research, 141980 Dubna, Russia*

⁹*Institut für Kernphysik, Goethe-Universität, 60438 Frankfurt, Germany*

¹⁰*Excellence Cluster 'Origin and Structure of the Universe', 85748 Garching, Germany*

¹¹*Physik Department E62, Technische Universität München, 85748 Garching, Germany*

¹²*II. Physikalisches Institut, Justus Liebig Universität Giessen, 35392 Giessen, Germany*

¹³*Institute for Nuclear Research, Russian Academy of Science, 117312 Moscow, Russia*

¹⁴*Institute of Theoretical and Experimental Physics, 117218 Moscow, Russia*

¹⁵*National Research Nuclear University MEPhI (Moscow Engineering Physics Institute), 115409 Moscow, Russia*

¹⁶*Department of Physics, University of Cyprus, 1678 Nicosia, Cyprus*

¹⁷*Laboratoire de Physique des 2 infinis Irène Joliot-Curie, Université Paris-Saclay, CNRS-IN2P3., F-91405 Orsay, France*

¹⁸*Nuclear Physics Institute, The Czech Academy of Sciences, 25068 Rez, Czech Republic*

¹⁹*LabCAF. F. Física, Univ. de Santiago de Compostela, 15706 Santiago de Compostela, Spain*

²⁰*Uniwersytet Warszawski, Wydział Fizyki, Instytut Fizyki Doświadczalnej, 02-093 Warszawa, Poland*

²¹*Dipartimento di Fisica and INFN, Università di Torino, 10125 Torino, Italy*

^a also at Coimbra Polytechnic - ISEC, Coimbra, Portugal

^b also at Technische Universität Dresden, 01062 Dresden, Germany

^c also at Frederick University, 1036 Nicosia, Cyprus

[†] deceased

(Dated: December 14, 2021)

Flow coefficients v_n of the orders $n = 1 - 6$ are measured with the High-Acceptance DiElectron Spectrometer (HADES) at GSI for protons, deuterons and tritons as a function of centrality, transverse momentum and rapidity in Au+Au collisions at $\sqrt{s_{\text{NN}}} = 2.4$ GeV. Combining the information from the flow coefficients of all orders allows to construct for the first time, at collision energies of a

few GeV, a multi-differential picture of the angular emission pattern of these particles. It reflects the complicated interplay between the effect of the central fireball pressure on the emission of particles and their subsequent interaction with spectator matter. The high precision information on higher order flow coefficients is a major step forward in constraining the equation-of-state of dense baryonic matter.

Heavy-ion collisions in the center-of-mass energy range of $\sqrt{s_{NN}} \approx 1 - 10$ GeV provide access to the properties of strongly interacting matter at very high net-baryon densities, which also define the characteristics of astrophysical objects like neutron stars [1]. Important information on this form of matter, e.g. on its Equation-Of-State (EOS), can be inferred from the measurement of collective flow [2, 3]. The majority of the flow studies at SIS18 and AGS energies performed up to now were restricted to the analysis of directed and elliptic flow (for a review see [4–7]). These correspond to the first (v_1) and second (v_2) order coefficients of the Fourier decomposition [8] of the azimuthal angle ϕ distribution of emitted particles with respect to the orientation of the reaction plane (RP). The latter is defined by the beam axis \vec{z} and the direction of the impact parameter \vec{b} of the colliding nuclei, which is given by the RP angle Ψ_{RP} ¹. It has been shown that important information can be extracted from an analysis of higher order flow coefficients relative to Ψ_{RP} . For instance, a comparison of the proton v_3 measured by HADES with UrQMD transport model calculations indicates that in particular v_3 exhibits an enhanced sensitivity to the EOS of the hadronic medium [9, 10]. Other transport model calculations suggest that a non-vanishing fourth order coefficient (v_4) measured at center-of-mass energies of a few GeV can constrain the nuclear mean field at high net-baryon densities [11]. At high energies (RHIC and LHC) the measurements of higher order flow coefficients relative to the symmetry plane of identical order were decisive to determine the shear viscosity over entropy density η/s of QCD matter at high temperatures [12]. Attempts have also been made to extract η/s for dense hadronic matter at lower energies by employing transport models [13–16] or hydrodynamic approaches [17]. Since these studies did not converge on conclusive results yet, input from measurements of higher order flow coefficients at low energies will be essential to further constrain the theoretical descriptions. Important information can be derived from an analysis of the scaling properties of higher flow harmonics. Initial theoretical considerations suggested, e.g., a simple scaling of v_2 and v_4 as $v_4(p_t)/v_2^2(p_t) = 1/2$ for an ideal fluid scenario [18], while later measurements at RHIC [19, 20]

and LHC [21–23] have revealed a more complex behavior. In the few GeV center-of-mass energy range, the flow pattern is strongly affected by the presence of slow spectator nucleons. They interfere with the particle emission from the central fireball and cause a distinct evolution of the relative contribution of odd and even flow harmonics as a function of rapidity [4, 7].

In this letter we report first measurements of higher order flow harmonics (i.e. v_n with $n = 3, 4, 5$ and 6) for protons, deuterons and tritons in fixed-target Au+Au collisions at $E_{beam} = 1.23A$ GeV, corresponding to a center-of-mass energy in the nucleon-nucleon system of $\sqrt{s_{NN}} = 2.4$ GeV.

The HADES experiment consists of six identical detection sections located between the coils of a toroidal superconducting magnet which each cover polar angles between 18° and 85° , corresponding to the center-of-mass pseudo-rapidity range $-0.79 < \eta_{cm} < 0.96$, and almost $\pi/3$ in azimuth. Each sector is equipped with a Ring-Imaging Cherenkov (RICH) detector followed by four layers of Multi-Wire Drift Chambers (MDCs), two in front of and two behind the magnetic field, as well as a Time-Of-Flight detector (TOF) ($44^\circ - 85^\circ$) and Resistive Plate Chambers (RPC) ($18^\circ - 45^\circ$). Hadrons are identified using the time-of-flight measured with TOF and RPC and the energy-loss information from TOF, as well as from the MDCs. Their momenta are determined via the deflection of the tracks in the magnetic field. The event plane (EP) angle is calculated from the emission angles and charges of projectile spectators as measured in the Forward Wall (FW) detector. It consists of 288 scintillator modules which are read out by photomultiplier tubes. The FW is placed at a 6.8 m distance from the target and covers the polar angles $0.34^\circ < \theta < 7.4^\circ$. The minimum bias trigger is defined by a signal in a $60 \mu\text{m}$ thick mono-crystalline diamond detector (START) [24], which is positioned in the beam line. In addition, on-line Physics Triggers (PT) are used based on hardware thresholds on the TOF signal corresponding to at least 5 (PT2) or 20 (PT3) hits in the TOF detector. By comparing the measured TOF+RPC hit multiplicity distribution with Glauber Model simulations it has been estimated that the PT3 trigger is selecting about 43 % (PT2 trigger: 72 %) of the total inelastic cross section of 6.83 ± 0.43 barn [25]. This multiplicity is also used for the offline centrality determination. For this analysis the PT3 triggered event sample is divided into four centrality intervals, each corresponding to 10 % of the total Au+Au cross section. A detailed description of the HADES experiment can be found in Ref. [26].

¹ In the following, $p_t = \sqrt{p_x^2 + p_y^2}$ is the transverse momentum and $y = 1/2 \ln[(E + p_z)/(E - p_z)]$ the rapidity of a given particle in the laboratory frame. The rapidity in the center-of-mass system is denoted by $y_{cm} = y - 1/2 y_{proj}$, with the projectile rapidity $y_{proj} = 1.48$.

Tracks are reconstructed using the hit information of the MDCs and Particle Identification (PID) is based on their time-of-flight. Protons, deuterons and tritons are selected within windows of $2.5 \cdot \sigma_\beta(p)$ width around the corresponding particle velocity β expected for a given momentum p . The resolutions $\sigma_\beta(p)$ also depend on p and are parameterized accordingly. To suppress contaminations to the particle sample identified via time-of-flight, in particular the ^4He contribution to the deuteron sample, the energy loss (dE/dx) measurements in the MDCs are used in addition. Phase space regions with a PID purity below 80 % are excluded from the analysis. In high multiplicity Au+Au collisions reconstruction efficiencies depend on the local track multiplicities. Since collective effects will cause anisotropies of the event shape, corresponding to local variations of the track densities and thus of the reconstruction efficiencies, a data-driven correction procedure depending on the track orientation relative to the EP is applied.

In the analysis presented here the azimuthal distributions of particle yields relative to the azimuthal orientation of the RP is used to determine the flow coefficients v_n [27–29]. However, as the azimuthal angle of the RP Ψ_{RP} is not accessible to measurements, an estimator for this angle, the EP angle Ψ_{EP} is introduced. For its determination hits of projectile spectators in the FW are used. From the laboratory angles ϕ_{FW} of the fired FW cells a vector $\vec{Q}_n = (Q_{n,x}, Q_{n,y}) = (\sum w \cos(n\phi_{FW}), \sum w \sin(n\phi_{FW}))$ of order n is calculated event-by-event. As weights the charges $w = |Z|$ are used, as determined from the signal height measured in a given FW cell. Non-uniformities in the FW acceptance and a possible misalignment of the beam are corrected by applying the standard re-centering method [29] to the positions X_{FW} and Y_{FW} by shifting the first moments $(\langle X_{FW} \rangle, \langle Y_{FW} \rangle)$ and dividing them by the second moments $(\sigma_{X_{FW}}, \sigma_{Y_{FW}})$. Residual non-uniformities in the EP angular distribution are removed by an additional flattening procedure [30]. The first order EP angle is then given by $\Psi_{\text{EP},1} = \arctan(Q_{1,y}/Q_{1,x})$. The flow coefficients of all orders discussed here are defined relative to $\Psi_{\text{EP},1}$, i.e. the first order EP measured via the spectator nucleons. This provides an estimate of the RP with the highest resolution. The flow coefficients v_n^{obs} are obtained from the event averages $v_n^{\text{obs}} = \langle \cos[n(\phi - \Psi_{\text{EP},1})] \rangle$. The EP resolution takes the dispersion of $\Psi_{\text{EP},1}$ relative to Ψ_{RP} into account, $v_n = v_n^{\text{obs}}/\mathfrak{R}_n$. This resolution, defined as $\mathfrak{R}_n = \langle \cos[n(\Psi_{\text{EP},1} - \Psi_{\text{RP}})] \rangle$, is determined according to Eq. 11 in Ref. [29]. Resulting values for the resolution for flow coefficients of different order n as function of the centrality are shown in Fig. 1.

Systematic uncertainties of the measured flow harmonics v_n result from systematic effects in the reconstruction and selection of charged tracks, in the PID procedures, and in the corrections applied to v_n . They are determined separately for each particle species, the or-

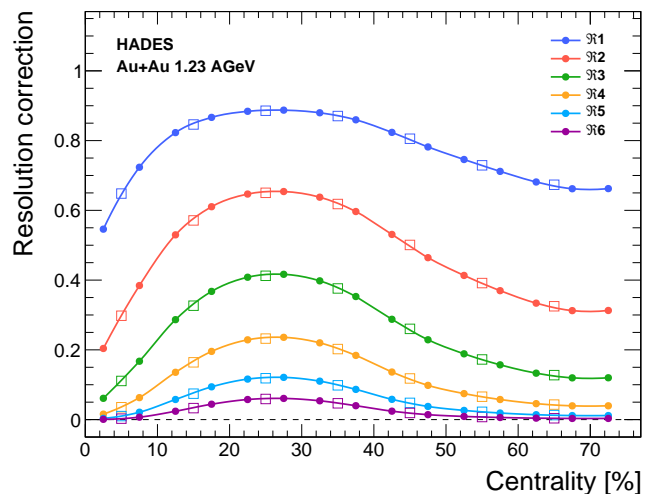


FIG. 1. The resolution of the first order spectator event plane \mathfrak{R}_n for the flow harmonics of different orders n as a function of the event centrality. The circles correspond to centrality intervals of 5 % width and the squares to 10 % width (curves are meant to guide the eye).

der n of the flow harmonics v_n , the centrality class and as a function of y_{cm} and p_t by varying selection criteria and parameters in the efficiency correction. Azimuthal asymmetries due to non-uniform acceptance and reconstruction efficiencies can cause additional systematic uncertainties. These are estimated by comparing the results obtained for a fully symmetric detector (i.e. six sectors) with those where different combinations of sectors are deliberately excluded from the analysis. It is found that the latter effect is mostly dominating in case of the odd flow coefficients, while for the even coefficients all of the above effects contribute roughly on the same level to the point-by-point systematic uncertainties. Furthermore, the analysis is performed on data recorded with a reversed magnetic field setting and for each day of data taking separately. No significant effects are observed in these cross-checks. A global systematic uncertainty arises from the EP resolution. This is mainly caused by so-called “non-flow” correlations which can distort the EP measurement. The magnitude of these systematic effects was evaluated using the three-subevent method, i.e. by determining the EP resolution for combinations of different sub-events separated in rapidity, and found to be below 5 % for the centralities 10 – 40 %.

Figures 2 and 3 present an overview of the measured values for v_1 to v_6 for protons, deuterons and tritons. Here only the values for semi-central (20 – 30 %) Au+Au collisions are shown as the effect of the event plane resolution corrections are smallest for this centrality range. Presented is the p_t dependence of the flow coefficients around mid-rapidity for v_2 , v_4 and v_6 , respectively at backward rapidity for v_1 , v_3 and v_5 , and their y_{cm} dependence for values averaged over the given p_t interval. The

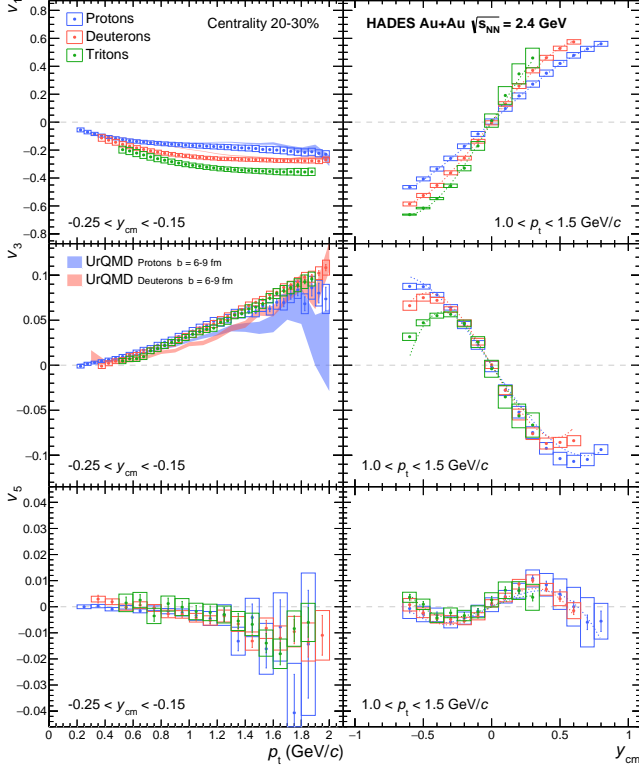


FIG. 2. The odd flow coefficients v_1 , v_3 and v_5 for protons, deuterons and tritons in semi-central (20 – 30 %) Au+Au collisions at $\sqrt{s_{NN}} = 2.4$ GeV. The left column displays the p_t dependence of v_1 (upper row), v_3 (middle row) and v_5 (lower row) in the rapidity interval $-0.25 < y_{cm} < -0.15$. In the right column the corresponding y_{cm} dependences are presented. The values are averaged over the p_t interval $1.0 < p_t < 1.5$ GeV/c. The dashed coloured curves represent fits to the data points (see text for details). Systematic errors are shown as open boxes. UrQMD model predictions for protons and deuterons are depicted as shaded areas [10].

latter has been fitted with the following functions to illustrate the symmetry of the measurements: $v_{1,3,5}(y_{cm}) = a_{1,3,5} y_{cm} + b_{1,3,5} y_{cm}^3$ and $v_{2,4,6}(y_{cm}) = c_{2,4,6} + d_{2,4,6} y_{cm}^2$. The values for odd flow coefficients (v_1 , v_3 and v_5) are consistent with zero at mid-rapidity, but exhibit a strong rapidity dependence, point-symmetric around $y_{cm} = 0$. Parameter v_1 develops a prominent mass dependence ($|v_1(p)| < |v_1(d)| < |v_1(t)|$) when moving away from mid-rapidity. For larger rapidity values a mass hierarchy is also observable for v_3 , which is, however, inverted with respect to v_1 ($|v_3(p)| > |v_3(d)| > |v_3(t)|$). In the case of v_5 , the sign of which is opposite to the one of v_3 , no mass hierarchy can be established due to the larger uncertainties. For v_2 around mid-rapidity a clear mass ordering can again be observed ($|v_2(p)| > |v_2(d)| > |v_2(t)|$) up to $p_t = 1.5$ GeV/c. This mass hierarchy becomes even more pronounced when moving away from mid-rapidity. A similar, though less significant, mass difference is visible for v_4 ($|v_4(p)| > |v_4(d)| > |v_4(t)|$). We note that

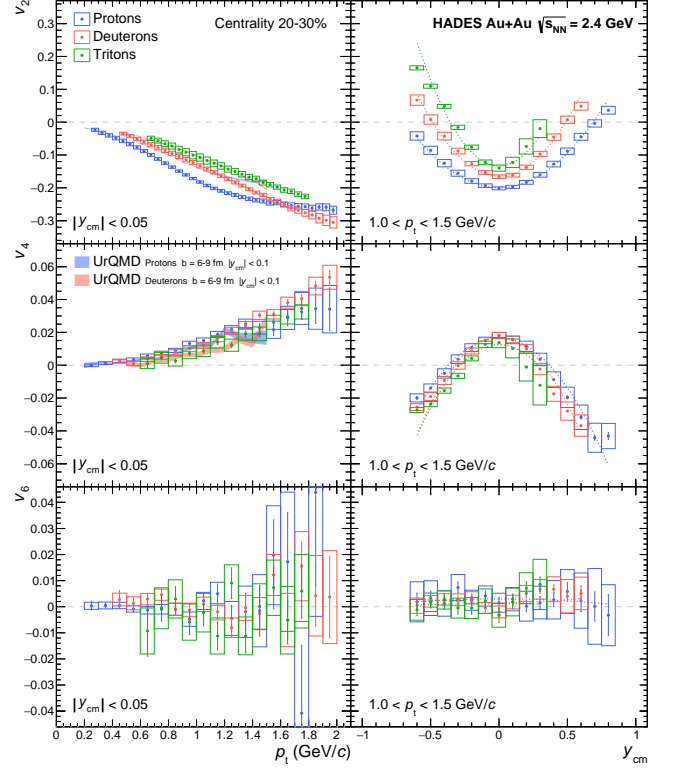


FIG. 3. The even flow coefficients v_2 , v_4 and v_6 for protons, deuterons and tritons in semi-central (20 – 30 %) Au+Au collisions at $\sqrt{s_{NN}} = 2.4$ GeV in the same representation as in Fig. 2, except that the p_t dependences are shown for the rapidity interval $|y_{cm}| < 0.05$.

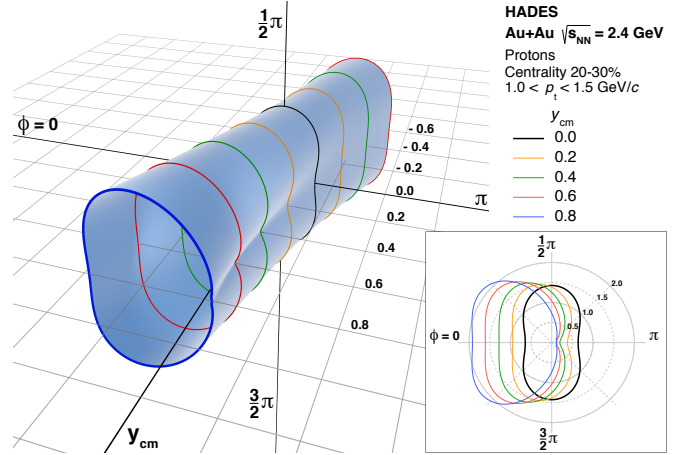


FIG. 4. A three-dimensional representation of the angular proton emission pattern, $1/\langle N \rangle (dN/d\phi)$, relative to the EP according to the flow coefficients of the orders $n = 1 - 6$, as parametrized by the fit functions shown in Figs. 2 and 3 for semi-central (20 – 30 %) Au+Au collisions. The shape corresponds to the ϕ dependent yield normalized by the ϕ averaged value, both integrated over the p_t interval $1.0 < p_t < 1.5$ GeV/c. The insert presents corresponding slices at different forward rapidities.

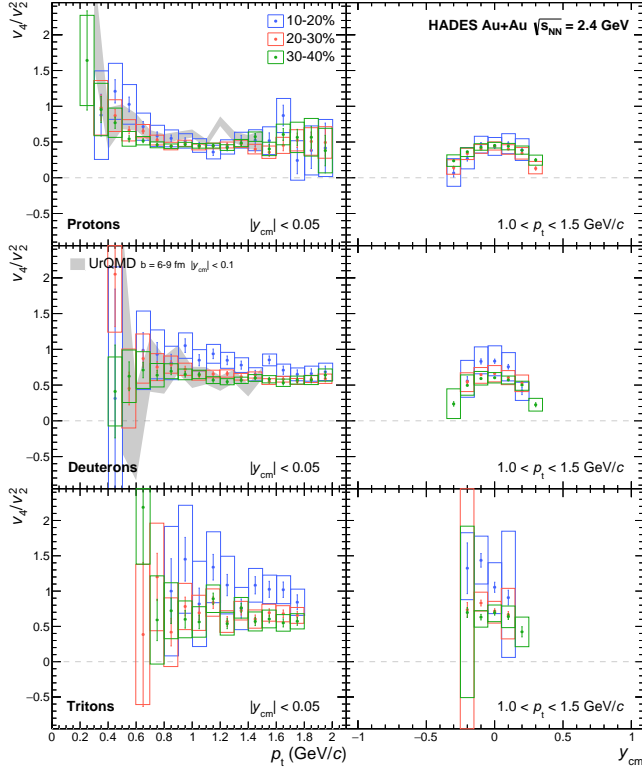


FIG. 5. The ratio v_4/v_2^2 for protons (upper row), deuterons (middle row) and tritons (lower row) in Au+Au collisions at $\sqrt{s_{NN}} = 2.4$ GeV for three different centralities. The left column displays the values as a function of p_t at mid-rapidity ($|y_{cm}| < 0.05$) and in the right column the values averaged over the interval $1.0 < p_t < 1.5$ GeV/c are shown as a function of rapidity. Systematic errors are represented by open boxes. UrQMD model predictions for protons and deuterons are depicted as shaded areas [10].

the integrated value for v_2 as measured here for protons agrees well with the world systematics, as compiled in [5, 31]. Also, we find the same p_t dependence of v_2 at mid-rapidity as observed by FOPI [32] and KaoS [33]. The UrQMD model is found to provide a good description of v_1 and v_4 of protons [10], while discrepancies between model and data can be observed in all other cases.

The multi-differential measurement of all flow coefficients up to order 6 allows to construct a three-dimensional picture of the angular particle emission pattern relative to the RP, as first proposed in Ref. [8], and is shown in Fig. 4 for the proton sample averaged over the interval $1.0 < p_t < 1.5$ GeV/c. It is constructed by inserting values of v_n for a given phase space interval from the parameterizations discussed above (see Figs. 2 and 3) into the cosine of the Fourier series: $1/\langle N \rangle (dN/d\phi) = 1 + 2 \sum v_n \cos(n\phi)$. At mid-rapidity, the combination of all flow coefficients results in a dipole shape centered around the beam axis with the odd coefficients being consistent with zero (see Fig. 2). The long axis of the elliptical shape is oriented along the $\phi = \pi/2$

direction, corresponding to out-of-plane emission. However, moving away from mid-rapidity a more asymmetric shape appears as the contribution of the odd coefficients increases. As a result, at very forward and backward rapidities the emission pattern develops a more triangular shape.

The ratio v_4/v_2^2 at mid-rapidity is shown in the left panels of Fig. 5. For protons a p_t independent value slightly below 0.5 is observed for the three centrality intervals shown here, while for deuterons and tritons it is found to be systematically above 0.5, both also without significant p_t dependence. However, these values are only reached around mid-rapidity as illustrated in the right panels of Fig. 5. A rapid drop of the ratio is observed for the considered particle types when moving away from mid-rapidity, as the y_{cm} distributions of v_2 and v_4 have different widths. Within the semi-central range between 10 % and 40 % no strong centrality dependence of the ratio v_4/v_2^2 is observed, as shown in Fig. 5. The transport model UrQMD is found to agree well with the measured values at mid-rapidity for protons and deuterons. It should also be investigated whether a description within the framework of hydrodynamic models is possible. However, as the expected values for η/s of dense baryonic matter will be relatively high [13, 14, 16, 17], any appropriate dynamical model is expected to be far away from an ideal fluid scenario. As the higher order flow harmonics are here measured relative to the first order RP, they are not related to initial state fluctuations as is the case for higher energies. Thus, the geometry of the reaction system at later stages will mainly determine the relative strength of the coefficients, which should also be reflected in other ratios, e.g. $v_3/(v_1 v_2)$. This ratio was studied as well, however, it was found to be dependent on p_t and particle type at backward rapidities, while around mid-rapidity no reliable determination was possible.

In summary, we report a multi-differential measurement of directed, v_1 , and elliptic flow, v_2 , and the first measurements of higher order flow coefficients ($v_3 - v_6$) for protons, deuterons and tritons in heavy-ion collisions in the few GeV center-of-mass energy regime. All flow coefficients are determined relative to a first order EP measured at projectile rapidities. It is found that away from mid-rapidity v_1 and v_5 have signs opposite to the one of v_3 , while similarly at mid-rapidity v_2 is negative and v_4 positive. Combining the flow coefficients $v_1 - v_6$ allows to construct for the first time a complete, multi-differential picture of the emission pattern of light nuclei as a function of rapidity and transverse momentum. For protons at mid-rapidity the ratio v_4/v_2^2 is found to be close to a value of 0.5, while it is slightly higher for deuterons and tritons. A strong rapidity dependence of this ratio is observed for all light nuclei. Theory calculations within a hydrodynamic framework, as e.g. described in [34–39], adapted to the description of baryon dominated matter are needed to investigate the question whether this kind

of matter exhibits a hydrodynamical behavior, at least in the last stages of the collision prior to freeze-out.

The collaboration gratefully acknowledges the support by SIP JUC Cracow, Cracow (Poland), National Science Center, 2016/23/P/ST2/04066 POLONEZ, 2017/25/N/ST2/00580, 2017/26/M/ST2/00600; TU Darmstadt, Darmstadt (Germany), VH-NG-823, DFG GRK 2128, DFG CRC-TR 211, BMBF:05P18RDFC1; Goethe-University, Frankfurt (Germany), BMBF:06FY9100I, BMBF:05P19RFFCA, GSI F&E, HIC for FAIR (LOEWE); Goethe-University, Frankfurt (Germany) and TU Darmstadt, Darmstadt (Germany), ExtreMe Matter Institute EMMI at GSI Darmstadt; TU München, Garching (Germany), MLL München, DFG EClust 153, GSI TMLRG1316F, BMBF 05P15WOFCA, SFB 1258, DFG FAB898/2-2; Russian Foundation for Basic Research (RFBR) funding within the research project no. 18-02-40086, National Research Nuclear University MEPhI in the framework of the Russian Academic Excellence Project (contract No. 02.a03.21.0005, 27.08.2013), Ministry of Science and Higher Education of the Russian Federation, Project "Fundamental properties of elementary particles and cosmology" No 0723-2020-0041; JLU Giessen, Giessen (Germany), BMBF:05P12RGGM; IPN Orsay, Orsay Cedex (France), CNRS/IN2P3; NPI CAS, Rez, Rez (Czech Republic), MSMT LM2015049, OP VVV CZ.02.1.01/0.0/0.0/16 013/0001677, LTT17003.

-
- [1] J. Adamczewski-Musch *et al.* (HADES), *Nature Phys.* **15**, 1040 (2019).
 - [2] P. Danielewicz, R. Lacey, and W. G. Lynch, *Science* **298**, 1592 (2002).
 - [3] A. Le Fèvre, Y. Leifels, W. Reisdorf, J. Aichelin, and C. Hartnack, *Nucl. Phys.* **A945**, 112 (2016).
 - [4] H. G. Ritter and R. Stock, *J. Phys.* **G41**, 124002 (2014).
 - [5] A. Andronic, J. Lukasik, W. Reisdorf, and W. Trautmann, *Eur. Phys. J.* **A30**, 31 (2006).
 - [6] N. Herrmann, J. P. Wessels, and T. Wienold, *Ann. Rev. Nucl. Part. Sci.* **49**, 581 (1999).
 - [7] W. Reisdorf and H. G. Ritter, *Ann. Rev. Nucl. Part. Sci.* **47**, 663 (1997).
 - [8] S. Voloshin and Y. Zhang, *Z. Phys.* **C70**, 665 (1996).
 - [9] P. Hillmann, J. Steinheimer, and M. Bleicher, *J. Phys.* **G45**, 085101 (2018).
 - [10] P. Hillmann, J. Steinheimer, T. Reichert, V. Gaebel, M. Bleicher, S. Sombun, C. Herold, and A. Limphirat, *J. Phys.* **G47**, 055101 (2020).
 - [11] P. Danielewicz, *Nucl. Phys.* **A673**, 375 (2000).
 - [12] U. Heinz and R. Snellings, *Ann. Rev. Nucl. Part. Sci.* **63**, 123 (2013).
 - [13] N. Demir and S. A. Bass, *Phys. Rev. Lett.* **102**, 172302 (2009).
 - [14] A. S. Khvorostukhin, V. D. Toneev, and D. N. Voskresensky, *Nucl. Phys.* **A845**, 106 (2010).
 - [15] B. Barker and P. Danielewicz, *Phys. Rev.* **C99**, 034607 (2019).
 - [16] J. B. Rose, J. M. Torres-Rincon, A. Schäfer, D. R. Oliinychenko, and H. Petersen, *Phys. Rev.* **C97**, 055204 (2018).
 - [17] Yu. B. Ivanov and A. A. Soldatov, *Eur. Phys. J.* **A52**, 367 (2016).
 - [18] N. Borghini and J.-Y. Ollitrault, *Phys. Lett.* **B642**, 227 (2006).
 - [19] J. Adams *et al.* (STAR), *Phys. Rev. Lett.* **92**, 062301 (2004).
 - [20] A. Adare *et al.* (PHENIX), *Phys. Rev. Lett.* **105**, 062301 (2010).
 - [21] G. Aad *et al.* (ATLAS), *Phys. Rev.* **C86**, 014907 (2012).
 - [22] S. Chatrchyan *et al.* (CMS), *JHEP* **02**, 088 (2014).
 - [23] S. Acharya *et al.* (ALICE), *JHEP* **07**, 103 (2018).
 - [24] J. Pietraszko, T. Galatyuk, V. Grilj, W. Koenig, S. Spataro, and M. Traeger, *Nucl. Instrum. Meth.* **A763**, 1 (2014).
 - [25] J. Adamczewski-Musch *et al.* (HADES), *Eur. Phys. J.* **A54**, 85 (2018).
 - [26] G. Agakishiev *et al.* (HADES), *Eur. Phys. J.* **A41**, 243 (2009).
 - [27] J.-Y. Ollitrault, *Phys. Rev.* **D48**, 1132 (1993).
 - [28] J.-Y. Ollitrault, *Nucl. Phys.* **A638**, 195 (1998).
 - [29] A. M. Poskanzer and S. A. Voloshin, *Phys. Rev.* **C58**, 1671 (1998).
 - [30] J. Barrette *et al.* (E877), *Phys. Rev.* **C56**, 3254 (1997).
 - [31] A. Andronic *et al.* (FOPI), *Phys. Lett.* **B612**, 173 (2005).
 - [32] W. Reisdorf *et al.* (FOPI), *Nucl. Phys.* **A876**, 1 (2012).
 - [33] D. Brill *et al.* (KaoS), *Z. Phys.* **A355**, 61 (1996).
 - [34] V. Russkikh, Y. Ivanov, Y. Pokrovsky, and P. Henning, *Nucl. Phys. A* **572**, 749 (1994).
 - [35] D. H. Rischke, Y. Pursun, J. A. Maruhn, H. Stoecker, and W. Greiner, *Acta Phys. Hung. A* **1**, 309 (1995).
 - [36] Yu. B. Ivanov, V. N. Russkikh, and V. D. Toneev, *Phys. Rev.* **C73**, 044904 (2006).
 - [37] I. Karpenko, P. Huovinen, H. Petersen, and M. Bleicher, *Phys. Rev. C* **91**, 064901 (2015).
 - [38] P. Batyuk, D. Blaschke, M. Bleicher, Yu. B. Ivanov, I. Karpenko, S. Merts, M. Nahrgang, H. Petersen, and O. Rogachevsky, *Phys. Rev.* **C94**, 044917 (2016).
 - [39] M. Martinez, M. D. Sievert, D. E. Wertepny, and J. Noronha-Hostler, (2019), arXiv:1911.12454 [nucl-th].